CHAPTER ONE

Stabilization of Hydrophilic Pores in Charged Lipid Bilayers by Anisotropic Membrane Inclusions

Ales Iglič[1,*], *and* Veronika Kralj-Iglič[2]

Contents

Abstract

We present theoretical and experimental evidences on stable pores in in the presence of anisotropic membrane inclusions. The model is based on minimization of free energy which involves three contributions: the energy due to the line tension of the lipid bilayer at the rim of the pore, the electrostatic energy of the charged membrane with the pore, and the energy of anisotropic membrane inclusions. In order to calculate the electrostatic energy of the membrane with the pore, the electric potential in the vicinity of an infinite, uniformly charged plate with a circular pore was calculated analytically. It is shown that the optimal pore size in the charged bilayer membrane is determined by the ionic strength of the surrounding electrolyte solution and by the intrinsic shape of the anisotropic membrane inclusions. Saddle-like membrane inclusions favor small pores whereas more wedge-like inclusions give rise to larger pore sizes [1]. For ionic strength bellow 0.05 mol/dm^3 the optimal size of the pore strongly increases with decreasing ionic strength. In accordance with theoretical predictions it was indicated experimentally

* Corresponding author. Tel.: +386 1 4250 278; Fax: +386 1 4768 850;
E-mail address: ales.iglic@fe.uni-lj.si (A. Iglič).

Advances in Planar Lipid Bilayers and Liposomes, Volume 6
ISSN 1554-4516, DOI 10.1016/S1554-4516(07)06001-2

that $C_{12}E_8$-induced anisotropic membrane inclusions may stabilize the hydrophilic pore in the membrane, presumably due to accumulation of $C_{12}E_8$ on toroidally shaped rim of the pore [2].

1. Introduction

The cell membrane is a semi-permeable barrier between the cell interior and its surroundings. One of the mechanisms for transmembrane transport involves the presence of pores in the lipid bilayer, through which a substantial flow of material can take place. For example, pores were observed in red blood cell ghosts [3–5], where the pore size depends on the ionic strength of the surrounding fluid [4].

The formation of pores in the membrane can be induced by application of high-intensity electric pulses of short duration [6]. This phenomenon is known as electroporation and has become widely used in medicine and biology [7–13]. A number of theoretical studies have been made to understand the physical basis of electroporation [14,15]. However, the mechanisms responsible for the energetics and stability of membrane pores still require further clarification.

The formation of hydrophilic pore in a lipid bilayer implies that lipid molecules near the edge of the pore rearrange themselves in a way that their polar head groups shield the hydrocarbon tails from the water [16,17]. In the model the excess energy due to modified packing of the phospholipid molecules at the edge of the pore is described by line tension, which makes the hydrophilic membrane pore energetically unfavorable. On the other hand, there are various examples where membrane pores live long enough to observe them experimentally [4,18,19]. The question arises what mechanisms could be responsible for stabilization of pores.

A possible mechanism has recently been suggested by Betterton and Brenner [20] for charged membranes, which is based on a competition between line tension and electrostatic repulsion between the apposed membrane rims within a pore. An analysis based on linearized Poisson–Boltzmann (PB) theory showed for certain combinations of model parameters the pore becomes energetically stabilized. However, the depth of the minimum is below kT (where k is Boltzmann's constant and T the absolute temperature) so that additional stabilizing effects are required to explain the existence of experimentally observed pores [20].

In this chapter we describe as a possible mechanism for the stabilization of pores in charged bilayer membranes, i.e., the non-homogeneous lateral distribution and orientational ordering of anisotropic membrane inclusions, i.e., their accumulation and orientation at the edge of the pore [1,2].

Anisotropic membrane inclusion may be a single molecule or a small complex of molecules (rigid or flexible) in biological or model membranes. If all in-plane orientations of anisotropic membrane component are not energetically equivalent, then the inclusion is referred to as anisotropic [21,22]. The inclusions may laterally distribute in such way as to minimize the membrane-free energy [21,23–28]. Besides the lateral distribution of membrane constituents in-plane orientational ordering of anisotropic inclusions has recently also been considered [22,29–31]. Non-

homogeneous lateral and orientational distributions of anisotropic membrane constituents are internal degrees of freedom. A method has been developed [21,32] starting from the microscopic description of the membrane constituents and applying methods of statistical physics to obtain the membrane-free energy. To obtain the equilibrium configuration of the membrane, the membrane-free energy is minimized taking into account the relevant geometrical constraints. The intrinsic properties of membrane constituents and interactions between them are thereby revealed in the equilibrium shape of the vesicle. Here we present this method while focusing on the effect of the intrinsic shape of anisotropic membrane inclusions on the equilibrium configuration of the membrane and the corresponding orientational ordering and lateral distribution of inclusions. The results presented may contribute to understanding the stability of pores in lipid bilayers.

Anisotropic membrane constituents are of special interest for the formation of membrane pores: the pore rim provides a geometry, which anisotropic inclusions favorably interact with [22,32–36]. Of particular interest in this respect are peptide [37–40] or detergent [2,41] stabilization of membrane pore. Detergents and certain antimicrobial peptides are amphipathic, often exhibiting their lytic activity [19,42,43], also through the formation of membrane pores. Antimicrobial peptides are typically elongated in shape, which renders their interaction with curved membranes highly anisotropic. Also the detergents or small complexes of the detergent with the surrounding membrane molecules may be anisotropic with the preference for high curvature of the pore rim due to their large hydrophilic part [2,43]. Examples for anisotropic membrane inclusions also include various lipids [44,45], glycolipids or lipoproteins [46], and gemini detergents [47].

We present the analysis of energetics of a single membrane pore in a binary lipid membrane, consisting of (charged) lipids and anisotropic inclusions [1,2]. The free energy of the inclusion-doped membrane contains the line tension contribution, the interaction energy between the anisotropic inclusions and the membrane, and the electrostatic energy of the charged lipids [1,2].

2. Geometrical Model of Hydrophilic Pore

We consider a planar lipid bilayer membrane that contains a single pore of aperture radius r, as schematically shown in Fig. 1. We locate a Cartesian coordinate system at the pore center with the axis of rotational symmetry (Z-axis) pointing normal to the bilayer midplane. Even though experimentally obtained evidence is currently not available, it seems a reasonable approximation to assume that the lipids within the rim assemble into a semi-toroidal configuration in order to shield the hydrocarbon chains from the contact with the aqueous environment. The bilayer thickness is $2b$.

A parameterization of the semi-toroidal pore is given by $x = b\cos\varphi\,((r/b) + 1 + \cos\theta)$, $\gamma = b\sin\varphi\,((r/b) + 1 + \cos\theta)$, and $z = b\sin\theta$ with $0 \le \varphi \le 2\pi$ and $\pi/2 \le \theta \le 3\pi/2$. The principal curvatures (for definition see Fig. 2) of the membrane in the region of the pore rim

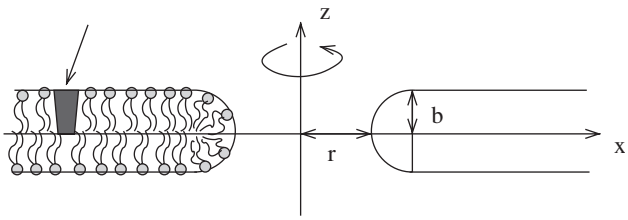

Figure 1 A planar lipid bilayer with a pore in the center. The figure shows the cross-section in the x–z plane. Rotational symmetry around the z-axis is indicated. On the left side, the packing of the lipid molecules is shown schematically. The head groups of lipid molecules are represented by filled circles. The arrow denotes the membrane inclusion which is shown schematically (adapted from [30]).

AU :1

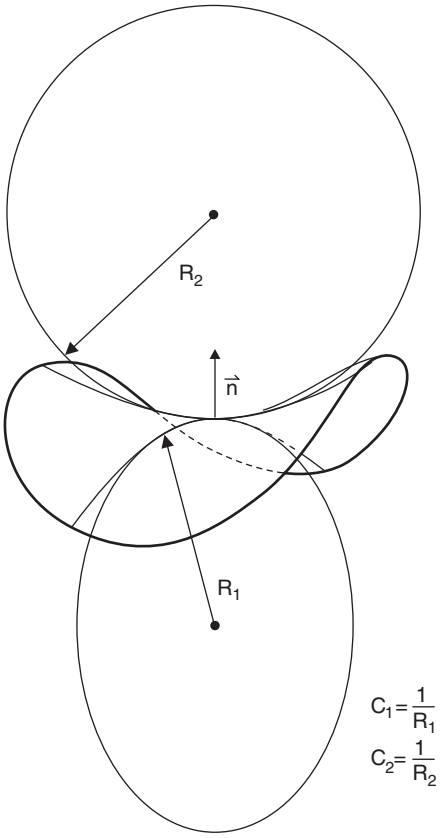

Figure 2 Definition of the two principal curvatures C_1 and C_2 (figure shows the saddle-like geometry).

$$c_1 = \frac{1}{b}, c_2 = \frac{\cos\theta}{r + b(1+\cos\theta)} \tag{1}$$

and the area element $dA_P = b[r + b(1 + \cos\theta)]d\varphi d\theta$. The local geometry within the rim is saddle-like everywhere, and most pronounced at $\theta = \pi$, where $c_1/c_2 = -r/b$. Note again, the semi-toroidal shape of the pore rim is an assumption; alternative pore shape could be considered but is not expected to alter the conclusions of the present work.

3. Free Energy of the System

To obtain the equilibrium size of the pore, the overall free energy, F, of the pore is minimized. We assume that F is the sum of three contributions:

$$F = W_{\text{edge}} + U_{\text{el}} + F_{\text{i}} \tag{2}$$

where W_{edge} is the energy due to the line tension of a lipid bilayer without the inclusions, U_{el} the electrostatic energy of the charged lipids, and F_{i} the energy due to the interactions between the membrane inclusions and the host membrane. We note that F is *excess* free energy, measured with respect to a planar, pore-free membrane [1].

For an inclusion-free membrane the energy W_{edge} is given by

$$W_{\text{edge}} = 2\pi\Lambda r \tag{3}$$

where r is the radius of the circular membrane pore and Λ the line tension (i.e., excess energy per unit length of the pore edge in the lipid bilayer. One can obtain a rough estimate for Λ on the basis of the elastic energy required to bend a lipid monolayer into a semi-cylindrical pore rim [2,16]. Adopting the usual quadratic curvature expansion for the free energy according to Helfrich [48] one finds [16] $\Lambda = \pi k_c/2b$ where k_c is the lipid layers's bending rigidity. For $b = 2.5$ m and $k_c = 10\ kT$ the values $\Lambda \approx 6\,kT/\text{nm} \approx 2 \times 10^{-11}$ J/m (at room temperature). This order of magnitude corresponds to experimental results for the line tension of lipid bilayers [18,49,50].

If rigid membrane inclusions are present within the membrane pore they replace some lipids. The replaced lipids do no longer contribute to the line tension W_{edge}. We shall account approximatively for this reduction in line tension by writing

$$W_{\text{edge}} = 2\Lambda(\pi r - N_{\text{P}} R_{\text{i}}) \tag{4}$$

where N_{P} denotes the number of inclusions within the pore rim and $2R_{\text{i}}$ the lateral extension of the cross-sectional shape of the inclusions. Steric interactions limit the number of inclusions within the membrane rim; $N_{\text{P}} \leq N_{\text{P}}^{\max} = \pi r/R_{\text{i}}$. Thus $W_{\text{edge}} \geq 0$, and the line tension always provides a tendency for the pore to shrink. AU :2

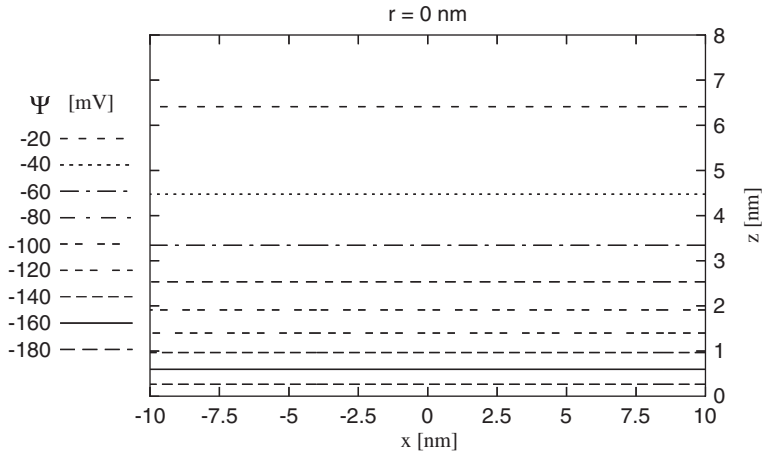

Figure 3 Equipotential surfaces in the vicinity of the charged plane in contact with the electrolyte solution. The values of the model parameters are: $\sigma = -0.05\ \mathring{\mathrm{A}}/\mathrm{m}^2$, $\varepsilon_w = 80$, $1/\kappa_\mathrm{d} = 2.8\ nm$ **(adapted from [52]).**

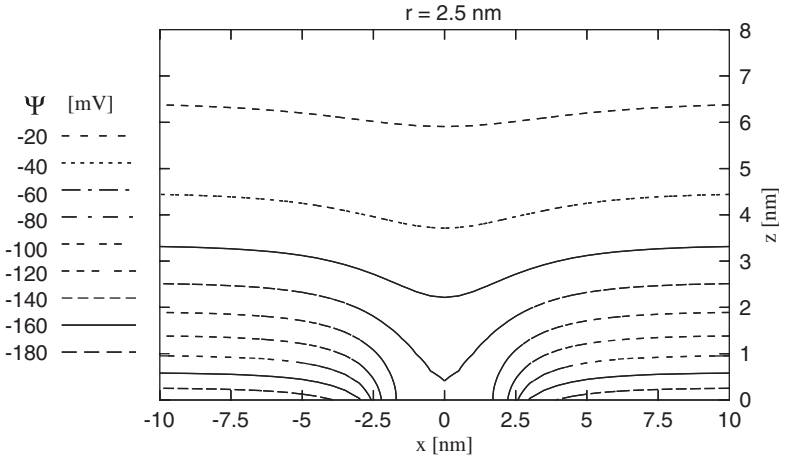

Figure 4 Equipotential surfaces in the vicinity of the charged plane with circular hole. The plane is in contact with the electrolyte solution. The radius of the circular pore (r) is 2.5 nm. The values of the model parameters are: $\sigma = -0.05\ \mathring{\mathrm{A}}/\mathrm{m}^2$, $\varepsilon_w = 80$, $1/\kappa_\mathrm{d} = 2.8\ nm$ **(adapted from [52]).**

4. Electrostatic Energy of the Pore

The calculation of the electrostatic energy of the membrane pore follows Betterton and Brenner [20] who have derived an expression valid for a very thin membrane ($b \to 0$) and within linearized PB theory. To keep our model traceable

we also adopt the result of linear PB theory where the equation

$$\nabla^2\phi = \kappa_d^2\phi \tag{5}$$

determines the (dimensionless) electrostatic potential $\phi = e_0\Psi/kT$ (electric potential Ψ is measured in mV) at given Debye length $l_D = \kappa_d^{-1}$:

$$\kappa_d = \sqrt{\frac{2n_0N_Ae_0^2}{\varepsilon_w\varepsilon_0kT}} \tag{6}$$

where ε_w is the dielectric constant of the aqueous solution, ε_0 the permittivity of free space, n_0 is the ionic strength of the surrounding electrolyte solution (i.e., bulk salt concentration; assuming a 1:1 salt such as NaCl), and N_A Avogadro's number and e_0 is the unit charge.

The solution of linearized PB (i.e., the electric potential Ψ_∞) for the case of infinite flat surface without a pore which satisfies the boundary conditions

$$\phi(z \to \infty) = 0 \tag{7}$$

$$\frac{\partial\phi}{\partial z}(z=0) = -\frac{\sigma}{\varepsilon_w\varepsilon_0} \tag{8}$$

can be written in the form [51]:

$$\phi_\infty(z) = \frac{\sigma}{\varepsilon_w\varepsilon_0\kappa_d}e^{-\kappa_d z} \tag{9}$$

where σ is the surface charge density. The solution of the linearized PB equation for planar lipid bilayer with the pore of radius r can be then written as the difference between the electrostatic potential of a flat infinite pore-free membrane (ϕ_∞) and the electrostatic potential of the circular flat membrane segment with the radius r (ϕ_p), both having constant surface charge density σ (Figs. 3 and 4) [52]: AU :3

$$\phi(x,z) = \phi_\infty(z) - \phi_p(x,z). \tag{10}$$

The electrical potential of circular flat membrane segment with the surface charge density σ and radius r is calculated using the cylindrical coordinates. For axisymmetric case the linearized PB equation in cylindrical coordinates reads:

$$\frac{1}{x}\frac{\partial}{\partial x}\left(x\frac{\partial\phi_p}{\partial x}\right) + \frac{\partial^2\phi_p}{\partial z^2} = \kappa_d^2\phi_p \tag{11}$$

where the origin of coordinate system is located at the pore center with the axis of rotational symmetry (z-axis) pointing normal to the bilayer midplane (Fig. 1). We seek for the solution of equation (11) by the ansatz

$$\phi_p(x,z) = R(x)Z(z) \tag{12}$$

where $R(x)$ is the function of x and $Z(z)$ the function of z. In this way equation (11) yields:

$$\frac{1}{R(x)}\frac{1}{x}\frac{\partial}{\partial x}\left(x\frac{\partial R(x)}{\partial x}\right)+\frac{1}{Z(z)}\frac{\partial^2 Z(z)}{\partial z^2}=\kappa_{\mathrm{d}}^2. \tag{13}$$

Since the first term in equation (13) depends solely on the coordinate x, while the second term is the function of coordinate z only, the sum of both terms can be always equal to the constant κ_{d}^2 only if both terms are also constant. We take

$$\frac{1}{Z(z)}\frac{\partial^2 Z(z)}{\partial z^2}=\kappa_{\mathrm{d}}^2+k^2 \tag{14}$$

$$\frac{1}{R(x)}\frac{1}{x}\frac{\partial}{\partial x}\left(x\frac{\partial R(x)}{\partial x}\right)=-k^2. \tag{15}$$

The general solution of equation (14) has the form [53]:

$$Z(z)=C\mathrm{e}^{-\sqrt{\kappa_{\mathrm{d}}^2+k^2}z}+C_1\mathrm{e}^{\sqrt{\kappa_{\mathrm{d}}^2+k^2}z}. \tag{16}$$

By taking into account the boundary condition $\phi(z\to\infty)=0$ we chose the value $C_1=0$ for the constant C_1 in equation (16), therefore:

$$Z=C\mathrm{e}^{-\sqrt{\kappa_{\mathrm{d}}^2+k^2}z}. \tag{17}$$

Equation (15) is rewritten in the form:

$$x^2\frac{\partial^2 R}{\partial x^2}+x\frac{\partial R}{\partial x}+k^2x^2R=0. \tag{18}$$

A regular solution of differential equation (18) is the Bessel function of the first kind [53]

$$R=CJ_0(kx). \tag{19}$$

The solution of equation (11) in the form of $\phi_{\mathrm{p}}(x,z)=R(x)Z(z)$ (see equation (12)) is therefore:

$$\phi_{\mathrm{p}}(x,z)=C(k)J_0(kx)\mathrm{e}^{-\sqrt{\kappa_{\mathrm{d}}^2+k^2}z}. \tag{20}$$

The *general* solution of equation (11) is thus:

$$\phi_{\mathrm{p}}(x,z)=\int_0^\infty \mathrm{d}kC(k)J_0(kx)\mathrm{e}^{-\sqrt{\kappa_{\mathrm{d}}^2+k^2}z}. \tag{21}$$

In the following equation (21) is first differentiated with respect to the coordinate z:

$$\frac{\partial\phi_{\mathrm{p}}}{\partial z}=\int_0^\infty \mathrm{d}k(-\sqrt{\kappa_{\mathrm{d}}^2+k^2})\,C(k)\,J_0(kx)\,\mathrm{e}^{-\sqrt{\kappa_{\mathrm{d}}^2+k^2}z}. \tag{22}$$

At $z=0$ it follows from above equation [52]:

$$\frac{\partial\phi_{\mathrm{p}}}{\partial z}|_{z=0}=\int_0^\infty \mathrm{d}k(-\sqrt{\kappa_{\mathrm{d}}^2+k^2})\,C(k)\,J_0(kx). \tag{23}$$

By using the Hankel transformation [53] the values of coefficients $C(k)$ can be calculated from equation (23) as follows:

$$C(k) = -\frac{k}{\sqrt{\kappa_d^2 + k^2}} \int_0^\infty \mathrm{d}x\, xJ_0(kx) \frac{\partial \phi_p}{\partial z}|_{z=0}. \quad (24)$$

The integration in equation (24) is divided in to two parts [52]:

$$C(k) = -\frac{k}{\sqrt{\kappa_d^2 + k^2}} \left(\int_0^r \mathrm{d}x\, xJ_0(kx) \frac{\partial \phi_p}{\partial z}|_{z=0} + \int_r^\infty dx\, xJ_0(kx) \frac{\partial \phi_p}{\partial z}|_{z=0} \right). \quad (25)$$

By taking into account the boundary conditions:

$$\frac{\partial \phi_p}{\partial z}(z=0) = -\frac{\sigma}{\varepsilon_w \varepsilon_0}, \quad x < r, \quad (26)$$

$$\frac{\partial \phi_p}{\partial z}(z=0) = 0, \quad x \geq r, \quad (27)$$

it follows:

$$C(k) = \frac{\sigma}{k\varepsilon_w \varepsilon_0 \sqrt{\kappa_d^2 + k^2}} \int_0^r \mathrm{d}(kx)\, kxJ_0(kx). \quad (28)$$

Considering the relations [53],

$$krJ_1(kr) = \int_0^r \mathrm{d}(kx) k\, xJ_0(kx), \quad (29)$$

it follows from equation (28):

$$C(k) = \frac{\sigma r J_1(kr)}{\varepsilon_w \varepsilon_0 \sqrt{\kappa_d^2 + k^2}}. \quad (30)$$

If the calculated expression for $C(k)$ is inserted in equation (21), the electric potential $\phi_p(x, z)$ can be written as [52]

$$\phi_p(x,z) = \frac{\sigma r}{\varepsilon_w \varepsilon_0} \int_0^\infty \mathrm{d}k \frac{J_0(kx)J_1(kr)}{\sqrt{\kappa_d^2 + k^2}} \mathrm{e}^{-\sqrt{\kappa_d^2 + k^2} z}, \quad (31)$$

where J_0 and J_1 are Bessel functions. By using equations (9), (??) and (31) we can determine the expression for electric potential of flat charged membrane with circular pore of radius r, being in contact with electrolyte solution [20] (Fig. 5): AU :4

$$\phi(x,z) = \frac{\sigma}{\varepsilon_w \varepsilon_0 \kappa_d} \mathrm{e}^{-\kappa_d z} - \frac{\sigma r}{\varepsilon_w \varepsilon_0} \int_0^\infty \mathrm{d}k \frac{J_0(kx)J_1(kr)}{\sqrt{\kappa_d^2 + k^2}} \mathrm{e}^{-\sqrt{\kappa_d^2 + k^2} z}. \quad (32)$$

The electrostatic-free energy [54] can be derived *via* a charging process [51,55]:

$$U_{\text{el, tot}} = 2\pi \int_0^\infty \sigma(x)\phi(z=0)\, x\, \mathrm{d}x. \quad (33)$$

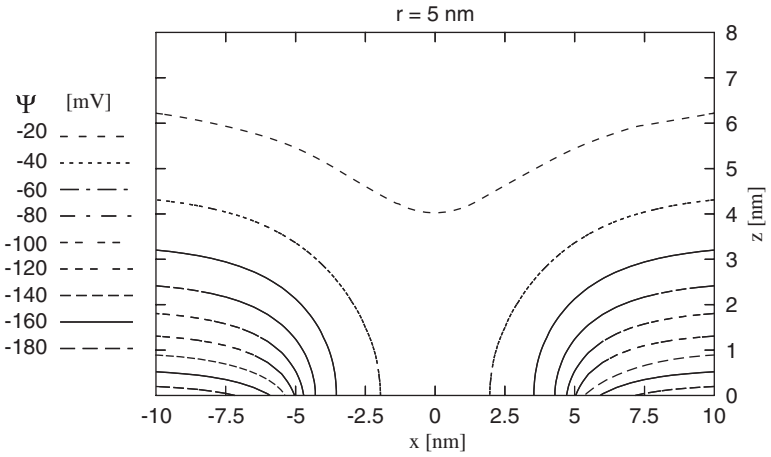

Figure 5 **Equipotential surfaces in the vicinity of the charged plane. The plane is in contact with the electrolyte solution. The radius of the circular pore (r) is 5 *nm*. The values of the model parameters are: $\sigma = -0.05$ Å$/\mathrm{m}^2$, $\varepsilon_w = 80$, $1/\kappa_\mathrm{d} = 2.8$ *nm* (adapted from [52]).**

Equation (33) is processed analytically by using equation (32). By subtracting the electrostatic energy of the charged pore-free membrane, one obtains an explicit expression for *excess* electrostatic energy of the pore [1,20]

$$U_\mathrm{el} = -\frac{\pi\sigma^2 r^2}{\varepsilon_\mathrm{w}\varepsilon_0\kappa_\mathrm{d}} + \frac{2\pi\sigma^2 r^3}{\varepsilon_\mathrm{w}\varepsilon_0}\int_0^\infty \frac{J_1(x)^2}{x\sqrt{x^2+\kappa_\mathrm{d}^2 r^2}}\,\mathrm{d}x. \tag{34}$$

5. Free Energy of the Inclusions

Any membrane constituent (single molecule or small complexes of molecules (Fig. 6)) may be treated as membrane inclusion in a two-dimensional continuum curvature field imposed by other membrane constituents. To describe the corresponding free energy, F_i, we use a phenomenological model [32,36,56] where the single-inclusion energy derives from the mismatch between the effective intrinsic shape of the inclusions and the actual shape of the membrane at site of the inclusions. The actual shape of the membrane at the site of the inclusion can be described by the diagonalized curvature tensor $\mathbf{C}$,

$$\mathbf{C} = \begin{bmatrix} C_1 & 0 \\ 0 & C_2 \end{bmatrix}, \tag{35}$$

where C_1 and C_2 are the two principal curvatures (Fig. 2). The intrinsic shape of a given inclusion can be described by the diagonalized curvature tensor $\mathbf{C}_\mathrm{m}$ [32,36],

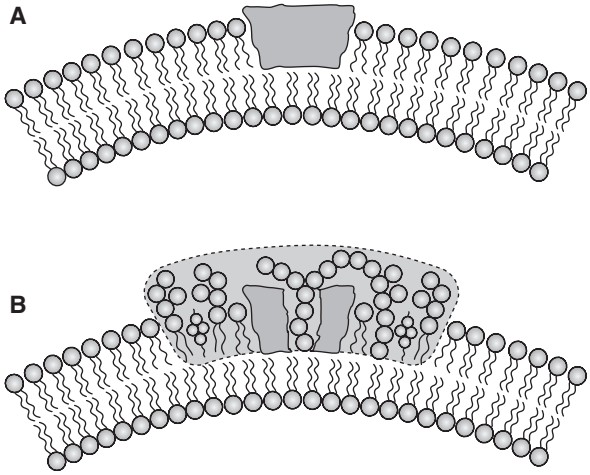

Figure 6 An inclusion can be a single molecule (A) [1] or small (flexible) complex of molecules (B) [60].

$$\mathbf{C}_{\mathrm{m}} = \begin{bmatrix} C_{1\mathrm{m}} & 0 \\ 0 & C_{2\mathrm{m}} \end{bmatrix}, \tag{36}$$

where $C_{1\mathrm{m}}$ and $C_{2\mathrm{m}}$ are two intrinsic principal curvatures of the inclusion (Fig. 7). The intrinsic principal curvatures are in general not identical. If they are identical ($C_{1\mathrm{m}} = C_{2\mathrm{m}}$), the intrinsic shape is isotropic (Fig. 7) and the in-plane orientation of the inclusion is immaterial. If $C_{1\mathrm{m}} \neq C_{2\mathrm{m}}$ the inclusion is called "anisotropic" (Fig. 7) [22,33,36,44,47].

The principal directions of the tensor $\mathbf{C}$ deviate in general from the principal directions of the tensor $\mathbf{C}_{\mathrm{m}}$; say, a certain angle ω quantifies this mutual rotation. The single-inclusion energy (E_{i}) can then be expressed in terms of the two invariants (trace and determinant) of the mismatch tensor $\mathbf{M} = \mathbf{R}\mathbf{C}_{\mathrm{m}}\,\mathbf{R}^{-1} - \mathbf{C}$ where $\mathbf{R}$ is the rotation matrix [56]

$$\mathbf{R} = \begin{bmatrix} \cos\omega & -\sin\omega \\ \sin\omega & \cos\omega \end{bmatrix}. \tag{37}$$

Terms up to second order in the elements of the tensor $\mathbf{M}$ are taken into account [32,56,57]:

$$E_{\mathrm{i}} = \frac{K}{2}(\mathrm{Tr}\mathbf{M})^2 + \bar{K}\,\mathrm{Det}\,\mathbf{M}, \tag{38}$$

where K and $\bar{K}$ are the constants of interaction between the inclusion and the surrounding membrane. Using equations (35–38), the single-inclusion energy (E_{i}) can be written in the form [32,36]:

$$E_{\mathrm{i}} = (2K + \bar{K})\,(H - H_{\mathrm{m}})^2 - \bar{K}\,(D^2 - 2DD_{\mathrm{m}}\,\cos(2\,\omega) + D_{\mathrm{m}}^2). \tag{39}$$

Quantities $H = (C_1 + C_2)/2$ and $H_{\mathrm{m}} = (C_{1\mathrm{m}} + C_{2\mathrm{m}})/2$ are the respective

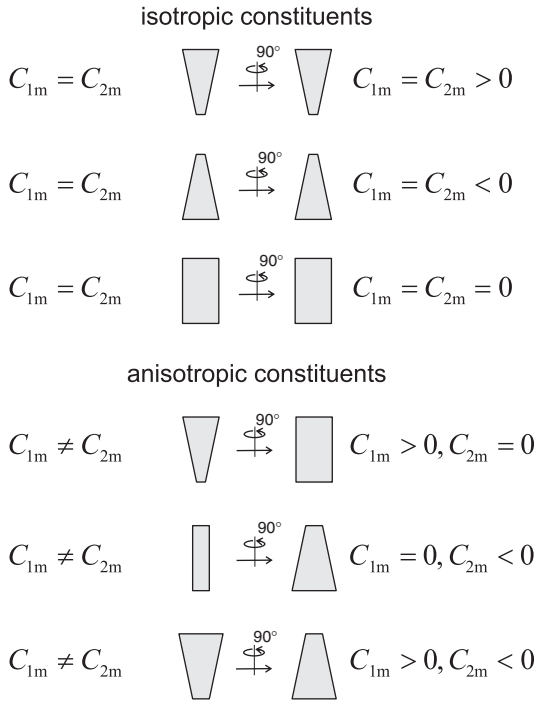

Figure 7 Schematic representation of different intrinsic shapes of some membrane constituents. Front and side views are shown. Upper: isotropic inclusion ($C_{1m} = C_{2m}$), lower: examples of anisotropic inclusions ($C_{1m} \neq C_{2m}$).

mean curvatures, while $D = |C_1 - C_2|/2$ and $D_m = |C_{1m} - C_{2m}|/2$ are the curvature deviators. The curvature deviator D_m describes the intrinsic anisotropy of the single membrane inclusion (Fig. 7) [28,32,36,44]. The phenomenological expression for the inclusion energy, E_i contains interaction constants K and $\bar{K}$ and intrinsic curvatures H_m and D_m that have been recently estimated for the special case of rigid anisotropic inclusion (Fig. 6A) [31]. In the case of more flexible membrane inclusions (Fig. 6B) the constants K, $\bar{K}$, H_m, and D_m have the meaning of local elastic constants and the spontaneous curvatures [57].

The inclusions can rotate around the axis defined by the membrane normal at the site of the inclusion. The time scale for orientational changes of the anisotropic inclusions is usually small compared to shape changes of the lipid bilayer. Therefore the corresponding partition function, q, of a single inclusion is [22,36,44]

$$q = \frac{1}{\omega_0} \int_0^{2\pi} \exp\left(-\frac{E_i(\omega)}{kT}\right) d\omega, \tag{40}$$

where ω_0 is an arbitrary angle quantum. Inclusions can also move laterally over the membrane bilayer, so that they can distribute laterally over the membrane in a way that is energetically the most favorable [33,36]. The lateral distribution of the

inclusions in a bilayer membrane of overall area A is in general non-uniform. Treating inclusions as point-like, independent, and indistinguishable, the expression for the contribution of the inclusions to the membrane-free energy can be derived, based on equations (39) and (40) [36]:

$$\frac{F_{\mathrm{i}}}{kT} = -N \ln\left[\frac{1}{A}\int_A q_{\mathrm{c}} I_0\left(\frac{2\bar{K}}{kT} D D_{\mathrm{m}}\right) \mathrm{d}A\right], \tag{41}$$

where N is the total number of inclusions in the membrane segment, while q_{c} is defined as

$$q_{\mathrm{c}} = \exp\left(-\frac{2K+\bar{K}}{kT}(H^2 - 2HH_{\mathrm{m}}) + \frac{\bar{K}}{kT} D^2\right), \tag{42}$$

and I_0 is the modified Bessel function. The integration in equation (41) is performed over the whole area of the membrane (A). For a large planar bilayer membrane that contains a single pore only those inclusions contribute to F_{i} that are located directly in the pore rim. In this case equation (41) can be rewritten in the form [1]:

$$\frac{F_{\mathrm{i}}}{kT} = n \int_{A_{\mathrm{P}}} \left[1 - q_{\mathrm{c}} I_0\left(\frac{2\bar{K}}{kT} D D_{\mathrm{m}}\right)\right] \mathrm{d}A_{\mathrm{P}}, \tag{43}$$

where $n = N/A$ is the average area density of the inclusions in the membrane, and where the integration extends only over the area, A_{p}, of the membrane rim. The influence of the inclusion's anisotropy (Fig. 7) is contained in the Bessel function $I_0(2DD_{\mathrm{m}}\bar{K}/kT)$. Because $I_0 \geq 1$ from equation (43) that anisotropy of inclusions always tends to lower F_{i}. Whether inclusions lower or increase F depends crucially on D_{m} and H_{m}, and on the interaction constants K and $\bar{K}$. The number of inclusions within the pore rim is [1]

$$N_{\mathrm{P}} = n \int_{A_{\mathrm{P}}} q_{\mathrm{c}} I_0\left(\frac{2\bar{K}}{kT} D D_{\mathrm{m}}\right) \mathrm{d}A_{\mathrm{P}}. \tag{44}$$

If inclusions have no preference for partition into the pore rim ($q_{\mathrm{c}} I_0 = 1$) then equation (44) predicts $N_{\mathrm{P}}/A_{\mathrm{P}} = n$. Combination of equations (43) and (44) yields [1]

$$\frac{F_{\mathrm{i}}}{kT} = nA_{\mathrm{P}} - N_{\mathrm{P}} \tag{45}$$

Hence, inclusions that enter the membrane pore (in density that exceeds the bulk density) contribute $1kT$ per inclusions to the free energy. If the density of the inclusions within the pore region greatly exceeds the bulk density then $nA_{\mathrm{P}} \ll N_{\mathrm{P}}$ and thus $F_{\mathrm{i}} \approx -N_{\mathrm{p}} kT$ [1]. The inclusion size determines the maximal number of inclusions, $N_{\mathrm{p}}^{\max}$ that can enter the pore rim. For rather large inclusions $R_{\mathrm{i}} \approx b$ and small pores $r \approx b$ we expect that $N_{\mathrm{p}}^{\max}$ is quite small, of the order of a very few inclusions [1]. This seems to indicate that F_{i} is hardly able to contribute to a substantial decrease in F. Below we show that nevertheless, for charged bilayer

membranes, anisotropic inclusions can dramatically reduce F (much more than $-N_p kT$).

We note that equation (39) with $D_m = 0$ has the same structure as the Helfrich-bending energy for isotropic membranes. The corresponding interaction constants, K and $\bar{K}$ for a lipid membrane could thus be determined [44] by $K = k_c a_0$ where $k_c \approx 10kT$ is the bending constant of a nearly flat lipid monolayer (that is part of a bilayer membrane) and $a_0 = 0.6-0.8\,\mathrm{nm}^2$ is the cross-sectional area per lipid.

We assume that $k_c a_0 \approx 10kT\,\mathrm{nm}^2$ is at least an order of magnitude smaller than the interaction constant K in expression for a single-inclusion energy (equation (39)) [1]. Hence, sufficiently large and anisotropic membrane inclusions are expected to strongly partition into "appropriately curved" membrane regions.

We note that partitioning of membrane inclusions into the rim of a membrane pore replace some structurally perturbed lipids (besides causing an extra (*excess*) splay). These lipids no longer contribute to the energy of the pore. The corresponding energy gain is not contained in F_i because we have taken it into account already in W_{edge} (see equation (2)).

6. Theoretical Predictions

All the following results are presented for a thickness of the lipid layer $b = 2.5\,\mathrm{nm}$, for a line tension of $\Lambda = 10^{-11}\,\mathrm{J/m}$, and for a surface charge density $\sigma = -0.05\,\mathrm{\AA/m}^2$ of the lipid layer [1]. Taking into account a cross-sectional area per lipid of $a_0 = 0.6-0.8\,\mathrm{nm}^2$ the value for σ would correspond roughly to a 1:4 mixture of (monovalent) charged and uncharged lipids. This is a common situation in biological and model bilayer membranes.

6.1. Inclusion-Free Membrane

In the case of inclusion-free membrane [20] the total membrane-free energy consists only of the line tension contribution (see equation 2) and the electrostatic-free energy (see equation (34)). The former favors shrinking, the latter widening (growing) of a membrane pore. For small values of Debye length l_D the pore closes, for large l_D the pore grows. Betterton and Brenner [20] have shown that for intermediate values of l_D there exists a very shallow local minimum of total membrane-free energy F as a function of the radius of the pore r. As an illustration, Fig. 8 shows the function $F(r)$ for three different values of l_D: 2.6 nm (a), 2.7 nm (b), and 2.8 nm (c). A local minimum of $F(r)$ is present only in curve (b). Figure 8 exemplifies a general finding for the inclusion-free isotropic and uniformly charged bilayer membrane: the local minimum of the membrane-free energy $F(r)$ is very shallow (below kT) and appears in a very narrow region of the values of the Debye length l_D. Based on these results it can be therefore concluded that the hydrophilic pore in isotropic and uniformly charged bilayer membrane cannot be stabilized solely by competition between the system electrostatic-free energy and the line tension energy of the pore rim [1,20].

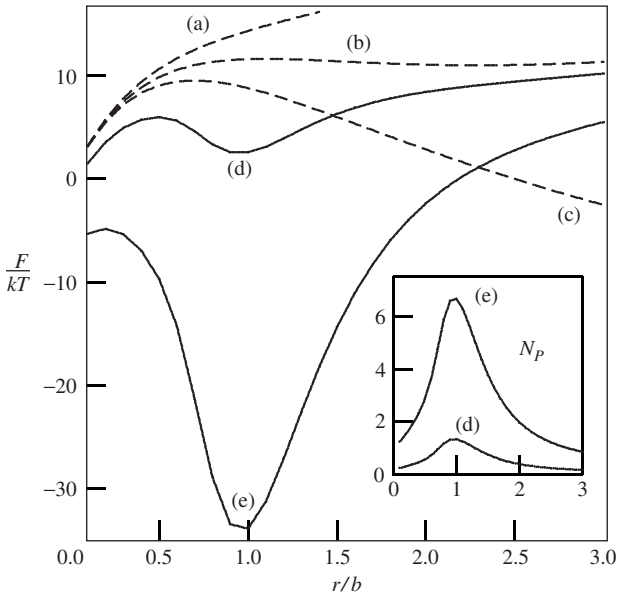

Figure 8 The pore-free energy, F, as a function of the pore size r [1]. The dashed lines correspond to a charged inclusion-free membrane of charge density of $\sigma = -0.05$ Å$/\mathrm{m}^2$ with Debye length $l_D = 2.6$ nm (a), $l_D = 2.8$ nm (b), and $l_D = 3.0$ nm (c). The solid lines describe the effect of adding anisotropic inclusions (characterized by $K = 50\ kT/\mathrm{nm}^2$, $\bar{K} = 35kT/\mathrm{nm}^2$, $c_{1m} = -c_{2m} = 1/b$) to the charged membrane with $\sigma = -0.1$ Å$/\mathrm{m}^2$ and $l_D = 2.8$ nm. The average area density of inclusions n is : $1/70000\ \mathrm{nm}^2$ (d) and $1/14000\ \mathrm{nm}^2$ (e). The inset shows the corresponding numbers, N_P, of inclusions within the membrane rim for curves (d) and (e) [1].

6.2. Influence of Anisotropic Intrinsic Shape of Membrane Inclusions

In order to illustrate the effect of anisotropy of the membrane inclusions we chose an inclusion which favors saddle shape $c_{1m} = -c_{2m} = 1/b$ (Fig. 7). Figure 8 shows $F(r)$ for two values of average area density of inclusions (n): $1/70000\ \mathrm{nm}^2$ (curve (d)) and $1/14000\ \mathrm{nm}^2$ (curve (e)). The ability of anisotropic inclusions to lower the local minimum of the membrane-free energy $F(r)$ can be clearly seen. The anisotropic inclusions tend to accumulate within the rim of the hydrophilic pore [1]. The number of inclusions within the rim of the pore (N_P) is estimated by equation (44). This number is plotted in the inset of Fig. 8 for $n = 1/70000\ \mathrm{nm}^2$ (d) and $n = 1/14000\ \mathrm{nm}^2$ (e).

The depth of the minimum of $F(r)$ for $n = 1/14000\ \mathrm{nm}^2$ (curve (e) in Fig. 8) is approximately $30\ kT$. It arises predominantly from the accumulation of the anisotropic membrane inclusions in the region of the pore rim. On the other hand, equation (45) predicts that the inclusion energy $F_i \approx N_P kT$. The inset of Fig. 8 shows that $N_P \leq 6$, therefore the deep minimum of $F(r)$ cannot arise solely from the inclusion contribution F_i [1]. To explain the deep minimum of $F(r)$ we recall that in the inclusion-free membrane the electrostatic energy and the line tension nearly balance each other for small enough values of r/b. If inclusions enter the pore

region they reduce the line tension (see equation (4)). As a result U_{el} is no longer counterbalanced by positive W_{edge} and thus strongly lowers the total membrane-free energy F [1].

The minimum of $F(r)$ in Fig. 8 occurs at $r \approx b$ (see curves (d) and (e)). This reflects our choice of the saddle shape of the anisotropic inclusion: $c_{1m} = 1/b$, $c_{2m} = -1/b$ (see also Fig. 7). In fact, for $r = b$ the principal curvatures of the pore rim at $\theta = \pi$ (see equation (1)) are $c_1 = 1/b$ and $c_2 = -1/b$, coinciding with the inclusion's principal curvatures. This observation suggests the possibility to increase the optimal size of the pore by altering the shape of the membrane inclusions from a saddle-like ($c_{1m} = 1/b$, $c_{2m} = -1/b$) towards a more wedge-like ($c_{1m} = 1/b$, $c_{2m} \approx 0$, see also Fig. 7) [1]. The smaller the magnitude of $|c_{2m}|$ the larger should the preferred pore size be (see also inset in Fig. 9). Regarding the principal curvatures at the waist of the rim, $c_1 = 1/b$ and $c_2 = -1/r$, one would expect that the optimal pore size (r^{opt}) is approximately determined by $c_{2m} = -1/r^{opt}$ and $c_{1m} = c_1 = 1/b$ leading to the approximative relation [1]

$$-\frac{c_{2m}}{c_{1m}} \approx \frac{b}{r^{opt}}. \tag{46}$$

In Fig. 9 [1] we consider anisotropic inclusions with intrinsic shape characterized by

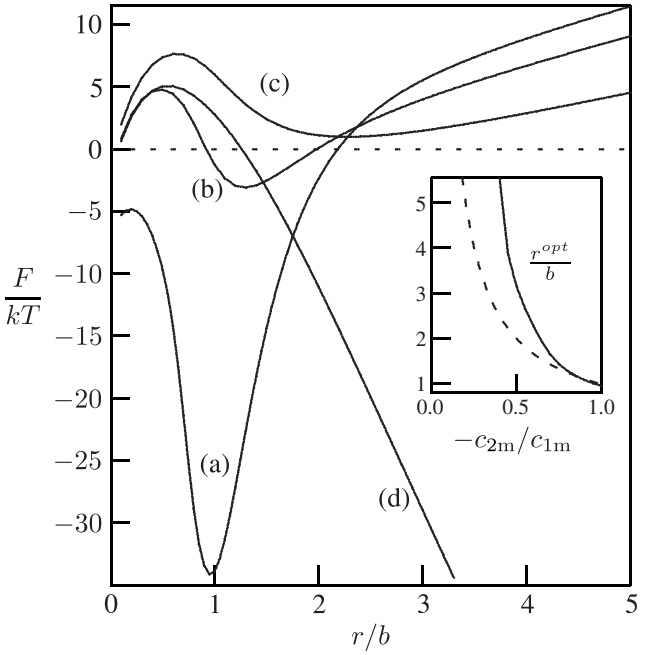

Figure 9 The pore-free energy, F, as a function of the pore size r for differently shaped, anisotropic inclusions: $c_{2m}/c_{1m} = -1$ **(a)**, $c_{2m}/c_{1m} = -0.8$ **(b)**, $c_{2m}/c_{1m} = -0.6$ **(c)**, and $c_{2m}/c_{1m} = 0$ **(d) [1]. In all cases the membrane is charged** ($\sigma = -0.05$ A/m^2, $l_D = 2.8$ nm), $c_{1m} = 1/b$ **and** $n = 1/14000$ nm^2. **The inset shows the position of the local minimum,** r^{opt}, **as a function of** c_{2m}/c_{1m} **(solid line). The dashed line in the inset corresponds to** $-c_{2m}/c_{1m} = b/r^{opt}$ **[1].**

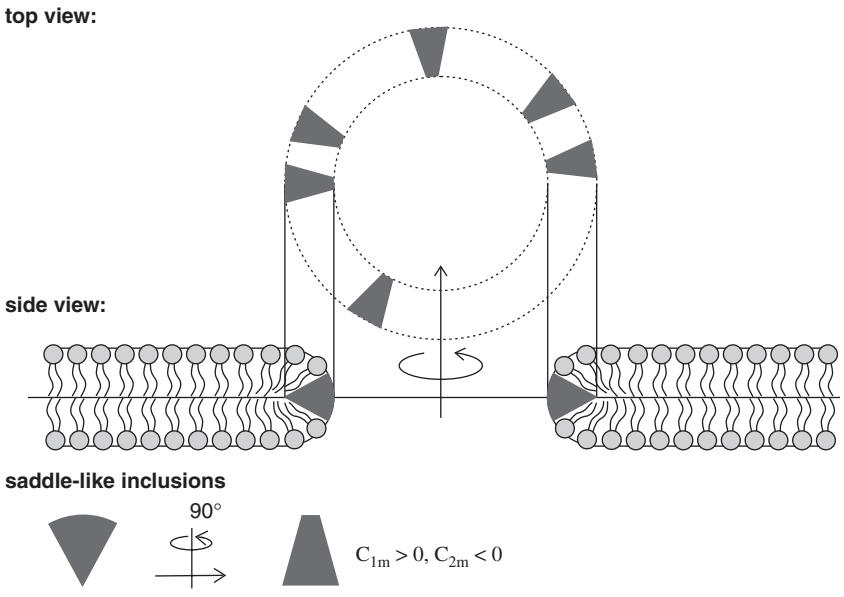

Figure 10 Schematic presentation of stabilization of hydrophilic pore in bilayer membrane by anisotropic saddle-like membrane inclusions.

$c_{1m} = 1/b$ and c_{2m}/c_{1m}: -1 (a), -0.8 (b), -0.6 (c), and 0 (d). As it can be seen in Fig. 9 the local minimum of $F(r)$ shifts to larger pore sizes as the inclusions become more wedge-shaped (compare the position of the local minimum of curves (a)–(c)). The solid line in the inset of Fig. 9 shows how the optimal pore radius r^{opt} changes with c_{2m}/c_{1m}. The broken line in the inset displays the prediction according to approximative equation (46). Figure 9 also shows that below some critical values of the ratio $|c_{2m}/c_{1m}|$ the local minimum in $F(r)$ disappears (in Fig. 9 for $|c_{2m}/c_{1m}| < 0.4$), which means that the pore becomes unstable and starts to grow in the process which never stops. It should be also stressed that for isotropic inclusions where $c_{1m} = c_{2m}$ (see Fig. 7) we do not find energetically stabilized pores. The stabilization of the pore derives from the matching of the rim geometry with the inclusion's preference (Fig. 10). The pore rim provides a saddle-like geometry with different signs of c_1 and c_2 (see also Fig. 2). Consequently a saddle-like inclusion geometry (that is, different signs of c_{1m} and c_{2m}) is needed to stabilize the pore [1].

6.3. Influence of Salt Concentration (Ionic Stregth)

In all examples presented in Fig. 9 we have added anisotropic inclusions to charged membranes with specifically selected Debye length $l_D = 2.8$ nm [1] (Debye length l_D is inversely proportional to square root of ionic strength n_0, see also equation (6)). We recall from Fig. 8 that this was the choice for which already an inclusion-free membrane exhibits a very shallow minimum in $F(r)$ (see dashed curve (b) in Fig. 8). The question arises whether pores in the membrane with anisotropic inclusions can

be stabilized also for other electrostatic conditions (i.e., other values of ionic strength). In this respect it is interesting to compare our theoretical predictions with experimental observation of stable pores in red blood cell ghosts for which data of the optimal pore radius r^{opt} as a function of the salt concentration n_0 exists [4]. Our theoretical approach [1] is able to reproduce these experimental data as presented in Fig. 11. Figure 11 shows the calculated and experimentally determined stable pore radius as a function of the salt concentration (ionic strength) in the suspension of red blood cell ghosts [1]. The inset of Fig. 11 shows the corresponding number of inclusions in the rim of the pore (N_{P}) (solid line) as well as the maximal possible number of inclusions in the rim of the pore $N_{\mathrm{P}}^{\max} = \pi r^{\mathrm{opt}}/R_{\mathrm{i}}$ (broken line) at which the inclusions would sterically occupy the entire rim. The observation $N_{\mathrm{P}} < N_{\mathrm{P}}^{\max}$ indicates applicability of our approach for the selected average area density of the inclusions in the membrane $n = 1/2000\ \mathrm{nm}^2$. Nevertheless, Fig. 11 should be understood only as illustration of the principal ability of anisotropic membrane inclusions to stabilize membrane pores, under different electrostatic conditions.

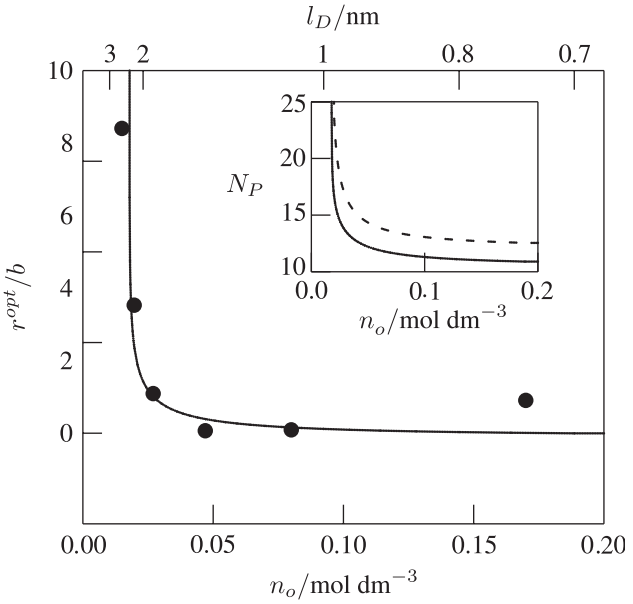

Figure 11 The optimal pore size r as a function of the ionic strength (salt concentration) of the surrounding electrolyte medium [1]. The charge density of the membrane is $\sigma = -0.05\ \mathrm{\AA/m^2}$, the average area density of the inclusions is $n = 1/2000\ \mathrm{nm}^2$, and the inclusion's preferred curvatures $c_{1\mathrm{m}} = 1/b$ and $c_{2\mathrm{m}}/c_{1\mathrm{m}} = -0.4$. Experimental values [4] are also shown (•). The inset shows the actual number of inclusions, N_{P}, residing in the pore of optimal size, r^{opt} (solid line), and the maximal number, $N_{\mathrm{P}}^{\max} = \pi r^{\mathrm{opt}}/R_{\mathrm{i}}$ (broken line) [1].

7. On the Role of Anisotropic Membrane Inclusions in Membrane Electroporation-Experimental Consideration

Electroporation is a method for artificial formation of pores in biological membranes by applying an electric field across the membrane [8–10]. A problem in the electroporation of living tissue is that it often causes irreversible damage to the exposed cells and tissue [12]. Increasing the amplitude of the electric field in electroporation diminishes cell survival rates [13]. On the other hand, if the applied electric field is too low, stable pores are not formed. A way to improve the efficiency of electroporation is chemical modification of the membranes by surfactants. Little is known about the effect of surfactants on cell membrane fluidity and its relation to electroporation.

A recent electroporation experiment has shown that nonionic surfactant (detergent) polyoxyethylene glycol $C_{12}E_8$ does not affect the reversible electroporation, however, it significantly increases the irreversible electroporation (i.e., irreversible electroporation occurs at lower applied voltage in the presence of $C_{12}E_8$ (Fig. 12) [2]). The addition of $C_{12}E_8$ caused cell death at the same voltage at which the reversible electroporation takes place. This can be explained by pore stabilization effect of $C_{12}E_8$ [2] taking into account the results of above presented theoretical study of the influence of anisotropic membrane inclusions on the energetics and stability of hydrophilic membrane pores.

$C_{12}E_8$ incorporates in lipid bilayer with polar detergent head group at the level of polar phospate head groups and with detergent chain inserted in between acyl chains of fatty acids of the membrane phospholipids (Thormond *et al.*, 1994). AU :6

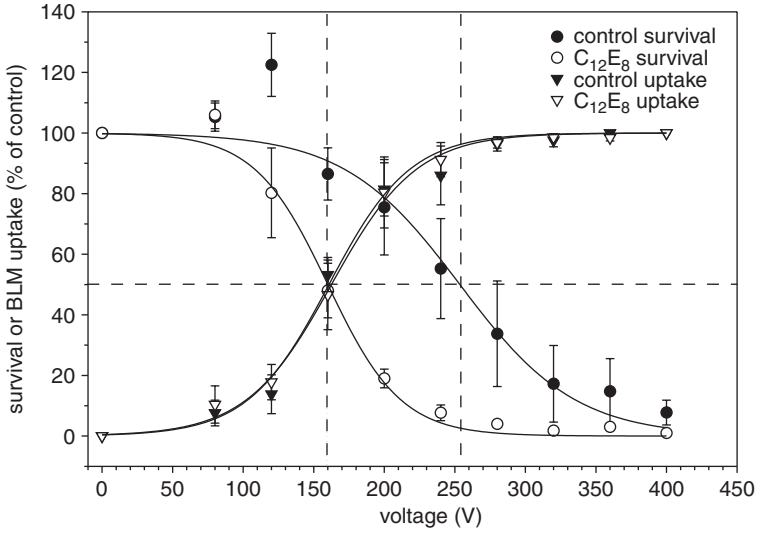

Figure 12 The effect of $C_{12}E_8$ on reversible electroporation (measured by bleomycin uptake) and irreversible electroporation measured by cell survival on cell line DC3F [2].

Incorporation of $C_{12}E_8$ into the phospholipid bilayer leads to decreased average chain length and increased average area per chain and considerable perturbation of acyl chain ordering of neighboring phospholipid molecules. Consequently, the effective shape of phospholipids around $C_{12}E_8$ changes from cylinder to inverted truncated cone (Thurmond *et al.*, 1994). A cooperative interaction of one $C_{12}E_8$ molecule and some adjacent phospholipid molecules has been proposed (Heerklotz *et al.*, 1998). Based on these experimental data an anisotropic effective shape of $C_{12}E_8$ phospholipids complex (inclusion) has been suggested recently [32,43,61].

In accordance with our theoretical predictions (Figs. 8 and 9) we therefore suggested that $C_{12}E_8$ induce anisotropic membrane inclusions [43] which stabilize the membrane hydrophilic pore by accumulating on toroidally shaped rim of the pore and attaining favorable orientation (Fig. 10) [2].

We presume that hydrophilic pores are formed at the voltages at which reversible electroporation takes place and that these pores are prerequisite for the bleomycin access to the cell interior that causes cell death. On the other hand, cell death that is a consequence of irreversible electroporation *is caused by electric field itself that provokes irreversible changes in the membrane*. In control cells, which were treated with $C_{12}E_8$ so that the pore stabilization did not occur, 50% of the cells survived the application of pulses of the amplitude of 250 V. In these cells, a resealing of the cell membrane took place while in the $C_{12}E_8$-treated cells no cells survived the application of pulses of the amplitude of 250 V, as resealing was prevented by $C_{12}E_8$ (Fig. 12). In control cells, we observed 50% of the permeabilization as determined by bleomycin uptake at 160 V [2]. At the same voltage, in the $C_{12}E_8$-treated cells we observed 50% of the permeabilization and also only 50% of cell survival after treatment with electric field (Fig. 12). This shows that the irreversible electroporation of the $C_{12}E_8$-treated cells is shifted to the same voltage at which reversible electroporation occur. In other words, electropermeabilization in the presence of $C_{12}E_8$ becomes irreversible as soon as it occurs. These results lead to the conclusion that stabilization of the hydrophilic membrane pores by $C_{12}E_8$ was induced by anisotropic membrane inclusions (Figs. 8–10).

To confirm this conclusion we performed additional experiments [2]. Namely, from above described experiments with $C_{12}E_8$ we could not distinguish between the pore stabilization effect of the $C_{12}E_8$-induced anisotropic membrane inclusions (Fig. 10) and the possibility that $C_{12}E_8$ could be toxic when it has access to the cell interior. Therefore in these additional experiments the molecules of $C_{12}E_8$ were added after the application of the train of 8 electric pulses. It was shown that $C_{12}E_8$ was not cytotoxic when it gained access to the cell interior (Fig. 13), as after electroporation the cell membrane remains permeable for relatively small molecules such as $C_{12}E_8$ [2]. From these results we concluded [2] that the cell death observed in the previous experiments (Fig. 12) is caused by bleomycin which is transported into the cell through pores which are stabilized by $C_{12}E_8$ (see Fig. 10). Also it was concluded that in order to show this effect $C_{12}E_8$ has to be incorporated in the cell membrane prior to application of the electric pulses.

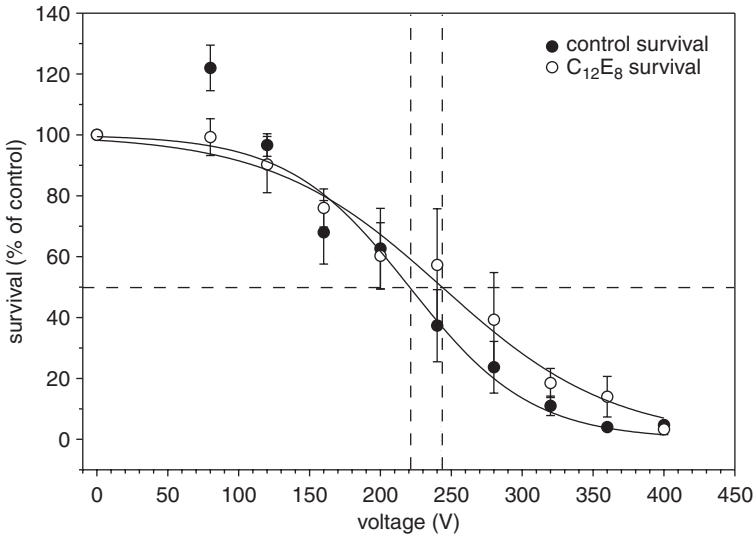

Figure 13 The effect of $C_{12}E_8$ added immediately after application of electric pulses on survival of DC3F cells [2].

8. Discussion and Conclusions

The influence that membrane inclusions have on the energetics of membrane pores is often interpreted in terms of altering the mezoscopic elastic properties of the membrane. For example, the effect of surfactants is often described by the surfactant dependent effective bending stiffness of a membrane bilayer and effective membrane spontaneous curvature [21,36,58,59]. In accordance it is assumed that the presence of cone-like or inverted cone-like membrane inclusions (see Fig. 7) can induce a shift in the spontaneous curvature [21,36,59]. This shift can be translated into a change of the line tension which may provide a simplified basis for analyzing the energetics of a membrane pore [18].

Our present theoretical approach contains isotropic inclusions only as a special case, namely the inclusions are isotropic for $D_m = 0$ (see also Fig. 7). Beyond the effect of cone-like and inverted cone-like inclusions, our present approach allows to analyze also other inclusion shapes, such as wedge-like or saddle-like (Fig. 7). Such inclusions can be characterized by an appropriate combination of H_m and D_m (or equivalently C_{1m} and C_{2m}).

In the case of *homogeneous lateral distribution* of membrane inclusions, the intrinsic spontaneous mean curvature of the inclusions (H_m) renormalize the membrane spontaneous curvature (see also [21,36,59]). However, if the lateral distribution of the inclusions is not homogeneous [21,29,36,60] the effect of the membrane inclusions (as for example surfactant-induced membrane inclusions, proteins, etc.) on membrane elasticity cannot be described simply by renormalization of membrane spontaneous curvature.

In the following we shortly discuss a few examples where we think that particularly the anisotropy of membrane-embedded inclusions could be relevant for the pore energetics.

Adding to the outer solution of the phospholipid membrane or the cell membrane a nonionic surfactant octaethyleneglycol dodecylether ($C_{12}E_8$) [2,41] causes a decrease of a threshold for irreversible electroporation (i.e., $C_{12}E_8$ decreases the voltage necessary for reversible electroporation) (Fig. 12). In other words, $C_{12}E_8$ molecules make transient pores in a membrane more stable [2]. In experiments the concentration of $C_{12}E_8$ was chosen so that it was not cytotoxic (Fig. 13) [2].

In order to explain the effect of $C_{12}E_8$ on reversible electroporation we suggested that $C_{12}E_8$-induced anisotropic membrane inclusions may stabilize the pore by accumulating on toroidal edge of the hydrophilic pore and by attaining a favorable orientation (Fig. 10). Our result could be thus considered as circumstantial evidence for the existence of hydrophilic pores that become stabilized by anisotropic membrane $C_{12}E_8$ inclusions that prevent membrane resealing.

Our theoretical approach could also help to better understand the pore energetics as recently investigated by Karatekin *et al.* [18]. For example, the authors have measured a dramatic increase of the transient pore lifetime induced by the detergent Tween 20 which has an anisotropic polar head group. The importance of the anisotropy of the polar heads of the detergents for the stability of anisotropic membrane structures has been indicated recently. It has been shown that a single-chained detergent with anisotropic dimeric polar head (dodecyl D-maltoside) may induce tubular nanovesicles [28,62] in a way similar as induced by strongly anisotropic dimeric detergents [47].

Our approach could add to better understanding of pore formation induced by some antimicrobial peptides [19,42]. These peptides have a pronounced elongated shape which arises from their alpha-helical backbone structure which renders them highly anisotropic. Some of these peptides are believed to cooperatively self-assemble into membrane pores. Thus, they can not only facilitate pore formation but they can *actively* induce it. Despite their importance there are currently only few theoretical investigations on the energetics of peptide-induced pore formation [37,38,40,63]. Our model provides a simple way to describe the underlying physics of peptide-induced pore formation in lipid membranes.

Our theoretical analysis of the stability and energetics of a single membrane pore is based on a simple and physically transparent model [1,2], which however involves a number of approximations.

As for example we have adopted a phenomenological expression for the membrane-inclusion interaction energy. This approach is (as in the Helfrich-bending energy [48]) valid if the local curvatures, C_1 and C_2, do not deviate too much from the preferred curvatures, C_{1m} and C_{2m}. On the other hand, the membrane rim provides local curvatures that differ greatly from those of the planar membrane. Hence, somewhere (either in the bulk membrane or within the rim) the deviations between the actual and the preferred curvatures are necessarily large. Yet, the Helfrich-bending energy describes well the line tension of an inclusion-free membrane (see for example [2]). On the same ground we are confident about the applicability of our expression for single-inclusion-free energy. There are also

approximations concerning the geometry of the membrane pore. Its shape is assumed to be circular, covered by a semi-toroidal rim [1,2]. However, there could be an inclusion-induced change in the cross-sectional shape of the membrane rim. Therefore we have performed additional calculations where we have allowed for a semi-ellipsoidal shape of the membrane rim. The free energy was then minimized with respect to the corresponding aspect ratio. With this additional degree of freedom we found qualitatively the same results as with the semi-toroidal rim [1] presented in this chapter.

The statistical mechanical approach to derive the inclusion-free energy F_i (equation (41)) assumes point-like inclusions, which interact only through a mean curvature field. Direct interactions between the inclusions [34] (which can be included in our theoretical approach [60,64,65]) may become important for the inclusions distributed in the pore rim where the distance between neighboring inclusions can be very small.

Nevertheless, none of the employed approximations can detract from our principal conclusion: anisotropic membrane inclusions can stabilize the pores in bilayer membrane [1,2].

Our theoretical approach takes into account the anisotropy of the membrane inclusions which enables us to describe various inclusion shapes: cone-like, inverted cone-like, wedge-like and saddle-like inclusions (see Fig. 7). In the model, the lateral density of the anisotropic inclusions is not kept constant so the inclusions may be predominantly localized in the energetically favorable regions [29,60], such as pore edges. Our model is simple, however it provides a lucid framework to analyze the energetics of pore formation in bilayer membranes [1] due to exogeneously bound molecules such as for example the detergent sodium cholate [18], detergent $C_{12}E_8$ [2], or the protein talin [66].

REFERENCES

[1] M. Fošnarič, V. Kralj-Iglič, K. Bohinc, A. Iglič, S. May, Stabilization of pores in lipid bilayers by anisotropic inclusions, J. Phys. Chem. 107 (2003) 12519–12526.

[2] M. Kandušer, M. Fosnarič, M. Šentjurc, V. Kralj-Iglič, H. Hägerstrand, A. Iglič, D. Miklavčič, Effect of surfactant polyoxyethylene glycol ($C_{12}E_8$) on electroporation of cell line DC3F, Coll. Surf. A 214 (2003) 205–217.

[3] M.R. Lieber, T.L. Steck, Dynamics of the holes in human-erythrocyte membrane ghosts, J. Biol. Chem. 257 (1982) 1660–1666.

[4] M.R. Lieber, T.L. Steck, A description of the holes in human-erythrocyte membrane ghosts, J. Biol. Chem. 257 (1982) 1651–1659.

[5] V.L. Lew, S. Muallem, C.A. Seymour, Properties of the Ca^{2+}-activated K^+ channel in one-step inside–out vesicles from human red-cellmembranes, Nature 296 (1982) 742–744.

[6] I.G. Abidor, V.B. Arakelyan, L.V. Chernomordik, Y.A. Chizmadzhev, V.F. Pastushenko, M.R. Tarasevich, Electric breakdown of bilayer lipid-membranes. 1. Main experimental facts and their qualitative discussion, Bioelectrochem. Bioener. 6 (1979) 37–52.

[7] E. Neumann, A.E. Sowers, C.A. Jordan (Ed.), Electroporation and Electrofusion in Cell Biology, Plenum Press, New York, 1989.

[8] P. Kramar, D. Miklavčič, A. Maček-Lebar, Determination of lipid bilayer breakdown voltage by means of linear rising signal, Bioelectrochem. (in print) AU :7

[9] A. Maček-Lebar, G. Serša, S. Kranjc, A. Grošelj, D. Miklavčič, Optimisation of pulse parameters in vitro for in vivo electrochemotherapy, Anticancer Res. 22 (2002) 1731–1736.
[10] A. Maček-Lebar, G.C. Troiano, L. Tung, D. Miklavčič, Inter-pulse interval between rectangular voltage pulses affects electroporation threshold of artificial lipid bilayers, IEEE Trans. Nanobioscience 1 (2002) 116–120.
[11] M. Pavlin, M. Kandušer, M. Reberšek, G. Pucihar, F.X. Hart, R. Magjarevic, D. Miklavčič, Effect of cell electroporation on the conductivity of a cell suspension, Biophys. J. 88 (2005) 4378–4390.
[12] R.C. Lee, M.S. Kolodney, Electrical injury mechanisms-dynamics of the thermal response, Plast. Reconstr. Surg. 80 (1987) 663–671.
[13] H. Wolf, M.P. Rols, E. Boldt, E. Neumann, J. Teissie, Control by pulse parameters of electric field-mediated gene-transfer in mammalian-cells, Biophys. J. 66 (1994) 524–531.
[14] J.M. Crowley, Electrical breakdown of biomolecular lipid-membranes as an electromechanical instability, Biophys. J. 13 (1973) 711–724.
[15] H. Isambert, Understanding the electroporation of cells and artificial bilayer membranes, Phys. Rev. Lett. 80 (1998) 3404–3407.
[16] L.V. Chernomordik, M.M. Kozlov, G.B. Melikyan, I.G. Abidor, V.S. Markin, Y.A. Chizmadzhev, The shape of lipid molecules and monolayer membrane-fusion, Biochim. Biophys. Acta 812 (1985) 643–655.
[17] J.D. Litster, Stability of lipid bilayers and red blod cell membranes, Phys. Lett. 53 (1975) 193–194.
[18] E. Karatekin, O. Sandre, H. Guitouni, N. Borghi, P.H. Puech, F. Brochard-Wyart, Cascades of transient pores in giant vesicles: line tension and transport, Biophys. J. 84 (2003) 1734–1749.
[19] H.W. Huang, Action of antimicrobial peptides: two-state model, Biochemistry 39 (2000) 8347–8352.
[20] M.D. Betterton, M.P. Brenner, Electrostatic edge instability of lipid membranes, Phys. Rev. Lett. 82 (1999) 1598–1601.
[21] V. Kralj-Iglič, S. Svetina, B. Žekš, Shapes of bilayer vesicles with membrane embedded molecules, Eur. Biophys. J. 24 (1996) 311–321.
[22] J.B. Fournier, Nontopological saddle splay and curvature instabilities from anisotropic membrane constituents, Phys. Rev. Lett. 76 (1996) 4436–4439.
[23] V.S. Markin, Lateral organization of membranes and cell shapes, Biophys. J. 36 (1981) 1–19.
[24] E. Sackmann, Membrane bending energy concept of vesicle and cell shapes and shape transitions, FEBS Lett. 346 (1994) 3–16.
[25] P.B.S. Kumar, G. Gompper, R. Lipowsky, Budding dynamics of multicomponent membranes, Phys. Rev. Lett. 86 (2001) 3911–3914.
[26] R. Lipowsky, R. Dimova, Domains in membranes and vesicles, J. Phys. Condens. Matter 15 (2003) 531–545.
[27] M. Laradji, P.B.S. Kumar, Dynamics of domain growth in self-assembled fluid vesicles, Phys. Rev. Lett. 93 (2004) ; 1–4/198105.
[28] V. Kralj-Iglič, H. Hägerstrand, P. Veranič, K. Jezernik, B. Babnik, D.R. Gauger, A. Iglič, Amphiphile-induced tubular budding of the bilayer membrane, Eur. Biophys. J. 34 (2005) 1066–1070.
[29] A. Iglič, M. Fošnarič, H. Hägerstrand, V. Kralj-Iglič, Coupling between vesicle shape and the non-homogeneous lateral distribution of membrane constituents in Golgi bodies, FEBS Lett. 574/1–3 (2004) 9–12.
[30] V. Kralj-Iglič, B. Babnik, D.R. Gauger, S. May, A. Iglič, Quadrupolar ordering of phospholipid molecules in narrow necks of phospholipid vesicles, J. Stat. Phys. 121 (in print). AU :8
[31] M. Fošnarič, K. Bohinc, D.R. Gauger, A. Iglič, V. Kralj-Iglič, S. May, The influence of anisotropic membrane inclusions on curvature elastic properties of lipid membranes, J. Chem. Inf. Model. 45 (2005) 1652–1661.
[32] A. Iglič, V. Kralj-Iglič, Effect of anisotropic properties of membrane constituents on stable shapes of membrane bilayer structure, in: H. Ti Tien, A. Ottova-Leitmannova (Eds.), Planar Lipid Bilayers (BLMs) and their Applications, Elsevier, Amsterdam, 2003, pp. 143–172.

[33] V. Kralj-Iglič, S. Svetina, B. Žekš, Shapes of bilayer vesicles with membrane embedded molecules, Eur. Biophys. J. 24 (1996) 311–321.
[34] S. Marčelja, Lipid-mediated protein interactions in membranes, Biophys. Biochim. Acta. 455 (1976) 1–7.
[35] S. Leibler, D. Andelman, Ordered and curved meso-structures in membranes and amphiphilic films, J. Phys. (Paris) 48 (1987) 2013–2018.
[36] V. Kralj-Iglič, V. Heinrich, S. Svetina, B. Žekš, Free energy of closed membrane with anisotropic inclusions, Eur. Phys. J. 10 (1999) 5–8.
[37] A. Zemel, D.R. Fattal, A. Ben-Shaul, Energetics and self-assembly of amphipathic peptide pores in lipid membranes, Biophys. J. 84 (2003) 2242–2255.
[38] M.J. Zuckermann, T. Heimburg, Insertion and pore formation driven by adsorption of proteins onto lipid bilayer membrane-water interfaces, Biophys. J. 81 (2001) 2458–2472.
[39] M.M. Sperotto, A theoretical model for the association of amphiphilic transmembrane peptides in lipid bilayers, Eur. Biophys. J. 26 (1997) 405–416.
[40] J.H. Lin, A. Baumgaertner, Stability of a melittin pore in a lipid bilayer: a molecular dynamics study, Biophys. J. 78 (2000) 1714–1724.
[41] G.C. Troiano, L. Tung, V. Sharma, K.J. Stebe, The reduction in electroporation voltages by the addition of a surfactant to planar lipid bilayers, Biophys. J. 75 (1998) 880–888.
[42] Y. Shai, Mechanism of the binding, insertion and destabilization of phospholipid bilayer membranes by alpha-helical antimicrobial and cellnon-selective membrane-lytic peptides, Biochim. Biophys. Acta 1462 (1999) 55–70.
[43] H. Hägerstrand, V. Kralj-Iglič, M. Fošnarič, M. Bobrovska-Hägerstrand, L. Mrowczynska, T. Söderström, A. Iglič, Endovesicle formation and membrane perturbation induced by polyoxyethyleneglycolalkylethers in human erythrocytes, Biochim. Biophys. Acta 1665 (2004) 191–200.
[44] V. Kralj-Iglič, A. Iglič, G. Gomišček, F. Sevšek, V. Arrigler, H. Hägerstrand, Microtubes and nanotubes of a phospholipid bilayer membrane, J. Phys. A Math. Gen. 35 (2002) 1533–1549.
[45] A. Chanturiya, J. Yang, P. Scaria, J. Stanek, J. Frei, H. Mett, M. Woodle, New cationic lipids form channel-like pores in phospholipid bilayers, Biophys. J. 84 (2003) 1750–1755.
[46] V.V. Malev, L.V. Schagina, P.A. Gurnev, J.Y. Takemoto, E.M. Nestorovich, S.M. Bezrukov, Syringomycin E channel: a lipidic pore stabilized by lipopeptide, Biophys. J. 82 (2002) 1985–1994.
[47] V. Kralj-Iglič, A. Iglič, H. Hägerstrand, P. Peterlin, Stable tubular microexovesicles of the erythrocyte membrane induced by dimeric amphiphiles, Phys. Rev. E 61 (2000) 4230–4234.
[48] W. Helfrich, Elastic properties of lipid bilayers: theory and possible experiments, Z. Naturforsch. 28 (1973) 693–703.
[49] C. Taupin, M. Dvolaitzky, C. Sauterey, Osmotic-pressure induced pores in phospholipid vesicles, Biochemistry 14 (1975) 4771–4775.
[50] J.D. Moroz, P. Nelson, Dynamically stabilized pores in bilayer membranes, Biophys. J. 72 (1997) 2211–2216.
[51] E.J. Verwey, J.Th.G. Overbeek, Theory of Stability of Lyophobic Colloids, Elsevier Publishing Company, New York, 1948.
[52] A. Iglič, K. Bohinc, M. Daniel, T. Slivnik, Effect of circular pore on electric potential of charged plate in contact with electrolyte solution, Electrotecn. Rev. (Slovenia) 71 (2004) ; 260.
[53] G.B. Arfken, H.J. Weber, Mathematical Methods for Physicists, Academic Press, San Diego, 1995.
[54] V. Kralj-Iglič, A. Iglič, A simple statistical mechanical approach to the free energy of the electric double layer including excluded volume effect, J. Phys. II (France) 6 (1996) 477–491.
[55] D. Andelman, Electrostatic properties of membranes: the Poisson–Boltzmann theory, in: R. Lipowsky, E. Sackmann (Eds.), Structure and Dynamics of Membranes, Elsevier, Amsterdam, 1995, pp. 603–642.
[56] V. Kralj-Iglič, M. Remškar, G. Vidmar, M. Fošnarič, A. Iglič, Deviatoric elasticity as a possible physical mechanism explaining collapse of inorganic micro and nanotubes, Phys. Lett. A 296 (2002) 151–155.

[57] A. Iglič, B. Babnik, U. Gimsa, V. Kralj-Iglič, On the role of membrane anisotropy in the beading transition of undulated tubular membrane structures, J. Phys. A: Math. Gen. 38 (2005) 8527–8536.
[58] C.R. Safinya, E.B. Sirota, D. Roux, G.S. Smith, Universality in interacting membranes: the effect of cosurfactants on the interfacial rigidity, Phys. Rev. Lett. 62 (1989) 1134–1137.
[59] B. Božič, V. Kralj-Iglič, S. Svetina, Coupling between vesicle shape and lateral distribution of mobile membrane inclusions, Phys. Rev. E 73 (2006) ; 041915/1–11.
[60] H. Hägerstrand, L. Mrowczynska, U. Salzer, R. Prohaska, K.A. Michelsen, V. Kralj-Iglič, A. Iglič, Curvature dependent lateral distribution of raft markers in the human erythrocyte membrane, Mol. Membr. Biol. 23 (2006) 277–288.
[61] M. Fošnarič, M. Nemec, V. Kralj-Iglič, H. Häägerstrand, M. Schara, A. Iglič, Possible role of anisotropic membrane inclusions in stability of torocyte red blood cell daughter vesicles, Coll. Surf. B 26 (2002) 243–253.
[62] H. Hägerstrand, V. Kralj-Iglič, M. Bobrowska-hagerstrand, A. Iglič, Membrane skeleton detachment in spherical and cylindrical microexovesicles, Bull. Math. Biol. 61 (1999) 1019–1030.
[63] P.C. Biggin, M.S.P. Sansom, Interactions of alpha-helices with lipid bilayers: a review of simulation studies, Biophys. Chem. 76 (1999) 161–183.
[64] A. Iglič, V. Kralj-Iglič, Budding of liposomes-role of intrinsic shape of membrane constituents, in: A. Leitmannova-Liu, H. Ti Tien (Eds.), Advances in Planar Lipid Bilayers and Liposomes, Vol. 4, Elsevier, Amsterdam, 2006, pp. 253–279.
[65] V. Kralj-Iglič, P. Veranič, Curvature-induced sorting of bilayer membrane constituents and formation of membrane rafts, in: A. Leitmannova-Liu, H. Ti Tien (Eds.), Advances in Planar Lipid Bilayers and Liposomes, Vol. 5, Elsevier, Amsterdam, 2006.
[66] A. Saitoh, K. Takiguchi, Y. Tanaka, H. Hotani, Opening-up of liposomal membranes by talin, Proc. Natl. Acad. Sci. USA 95 (1998) 1026–1031.

AUTHOR QUERY FORM

ELSEVIER	**Book: ADPLAN-V006** **Chapter: 6001**	**Please eail or fax your responses and any corrections to:** **Eail:** **Fax:**

Dear Author,

During the preparation of your manuscript for typesetting, some questions may have arisen. These are listed below. Please check your typeset proof carefully and mark any corrections in the margin of the proof or compile them as a separate list*.

Disk use
Sometimes we are unable to process the electronic file of your article and/or artwork. If this is the case, we have proceeded by:
☐ Scanning (parts of) your article ☐ Rekeying (parts of) your article
☐ Scanning the artwork

Bibliography
If discrepancies were noted between the literature list and the text references, the following may apply:

☐ The references listed below were noted in the text but appear to be missing from your literature list. Please complete the list or remove the references from the text.
☑ *Uncited references:* This section comprises references that occur in the reference list but not in the body of the text. Please position each reference in the text or delete it. Any reference not dealt with will be retained inthis section

Queries and/or remarks

Location in Article	Query / remark	Response
AU:1	Has permission been obtained for all the figures? Please check.	
AU:2	'Of' has been changed to 'for' in the sentence "Thus...the pore to shrink." Please check.	
AU:3	Please check the citation of figures 3, 4 and 5.	
AU:4	Please provide the equation number in the sentence "By using equations (9), (??) and...solution..."	
AU:5	Does "7" in "see also 7" refer to figure 7? Please check.	
AU:6	Thormond et al (1994), Thurmond et al. (1994) and Heerklotz et al. (1998) are not listed. Please provide. As the numbered system is being	

	followed, please suggest if the references need to be renumbered after citation of these references in the text.	
AU:7	Please provide the volume number, page range and year of publication in Ref. 8.	
AU:8	Please provide the page range and year of publication in Ref. 30.	